

Cucurbit[8]uril Mediated Donor–Acceptor Ternary Complexes: A Model System for Studying Charge-Transfer Interactions

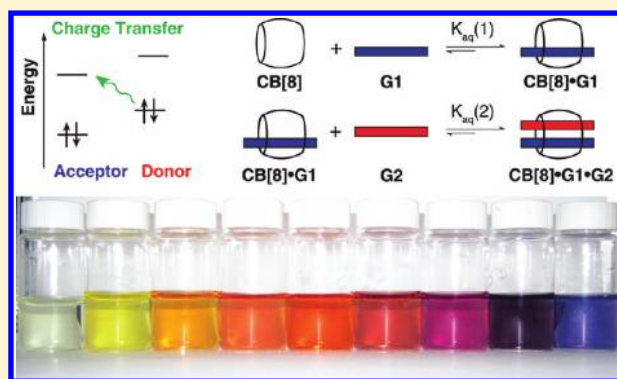
Frank Biedermann and Oren A. Scherman*

Melville Laboratory for Polymer Synthesis, Department of Chemistry, University of Cambridge, Lensfield Road, Cambridge CB2 1EW, United Kingdom

Supporting Information

ABSTRACT: A supramolecular self-assembly approach is described which allows for the convenient preparation of a wide range of charge-transfer (CT) donor–acceptor complexes in aqueous solutions. When one equiv of the macrocyclic host cucurbit[8]uril (CB[8]) is added to an aqueous donor and acceptor solution, a heteroternary complex forms inside the host's cavity with a well-defined face-to-face π – π -stacking geometry of the donor and acceptor. This heteroternary, CB[8]-mediated complex offers the opportunity to study the CT phenomena at low concentrations and free from complications arising from any donor–donor and acceptor–acceptor interactions as a result of the large binding affinities and the very high selectivity over the formation of these homoternary complexes. Thus, this supramolecular self-assembly strategy is a practical donor–acceptor

mix-and-match approach with synthetic advantages over much more cumbersome tethering schemes. While the characteristic UV/vis features of a few CB[8] ternary systems had been described as a CT band, we present for the first time systematic evidence for the existence of CT interactions between several donor–acceptor pairs that are mediated by the host CB[8]. Correlation of the experimentally obtained CT λ_{max} to computed HOMO–LUMO energies demonstrated that the CT process in the host's cavity can be described by the Mulliken model. Furthermore, the literature claim of a “CT driving force” for the formation of CB[8] ternary complexes was scrutinized and evaluated by calorimetric (ITC) and ESI-MS measurements. The findings indicated that neither in the aqueous medium nor in the “gas-phase” is CT of energetic relevance to the Gibbs free binding energy. In contrast, electrostatic considerations combined with solvation effects are much better suited to rationalize the observed trends in binding affinities. Additionally, the CT λ_{max} was found to be much more red-shifted (≥ 75 nm) inside the CB[8] cavity than in any polar organic solvents or water, indicating a significant stabilization of the CT excited state within the host cavity, further demonstrating the unique electrostatic, polar properties of the host cavity.



INTRODUCTION

Among the supramolecular binding forces, charge-transfer (CT) interactions can be considered the most controversial as they are likely the most easily identifiable interaction mode on account of characteristic features in electronic spectra, while their energetic contribution to the complex formation is often debatable. As CT effects are inherently quantum mechanical in nature, their experimental investigation and theoretical description remain challenging.^{1–7} Commonly, a simplified but still widely accepted model by Mulliken is utilized to explain the CT process, albeit the need for more sophisticated theoretical descriptions that incorporate relaxation effects have arisen in the past decade.^{8,9} A deep understanding of CT interactions is not only accompanied by theoretical advances but will subsequently benefit the design of systems that rely on physical charge separation (and subsequent migration) as in conducting polymers, in solar cells, for data storage applications, as well as in mimicry of nature's photosynthesis machinery.^{10–15} Furthermore, CT binding forces have also

been exploited for the synthesis of novel materials.^{16–20} While the majority of biological and artificial host–guest/receptor–substrate interactions can be understood in terms of electrostatic and polarization contributions, H-bonding, and solvation effects,^{21–26} some enzymatic catalysis pathways, however, crucially rely on CT interaction.^{27–29} Synthetic chemical transformations that depend on CT excitations have also been described.^{30–32}

The most simplistic way to study CT model systems is to mix a suitable donor and acceptor in solution and subsequently analyze the spectroscopic features of the spontaneously formed donor–acceptor complexes.³³ In this approach, however, the study is often hampered by the fact that the low binding strength of the donor to the acceptor as well as a small specific absorbance (compared to intramolecular light absorption

Received: November 15, 2011

Revised: January 26, 2012

Published: February 6, 2012

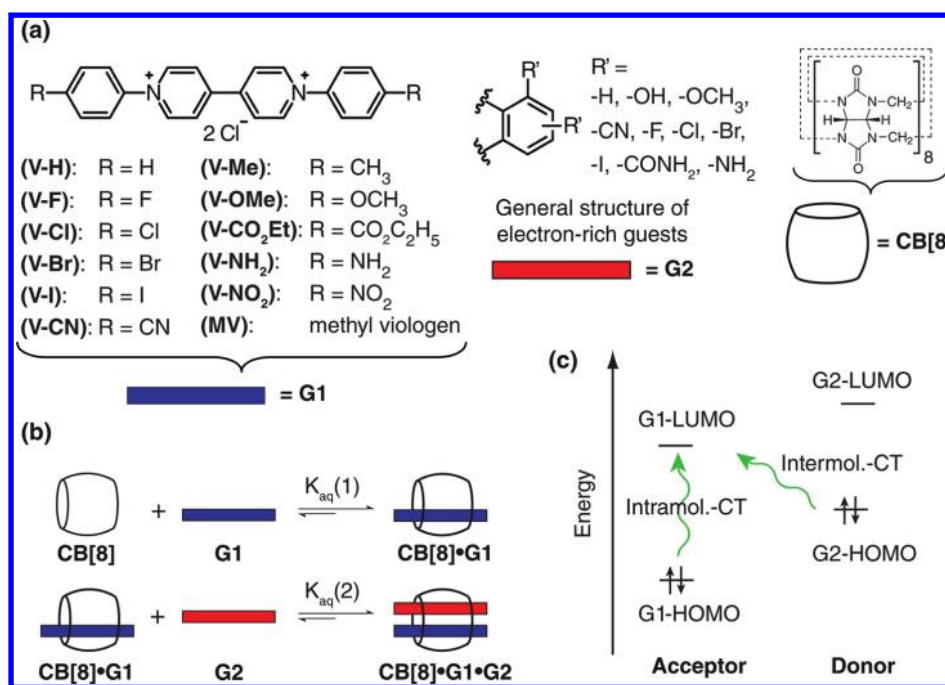


Figure 1. (a) Chemical structures of a wide range of electron-poor dicationic viologen first guest (G1) and electron-rich aromatic second guest (G2) binding simultaneously to the barrel-shaped macrocyclic host CB[8] in a 1:1:1 stoichiometry. (b) Stepwise formation of the ternary complexes in aqueous solutions. (c) Schematic energy diagram for the donor–acceptor interaction between G2 and G1 inside CB[8].

pathways) of the CT UV/vis band requires the use of high molar concentrations of both donor and acceptor components. Additionally, under these experimental conditions donor–donor and acceptor–acceptor electronic interactions such as excimer formations can occur, complicating the analysis significantly. Furthermore, different donor–acceptor geometries such as face-to-face or T-shape stacking of aromatic systems can be present which create additional drawbacks for the theoretical modeling of the experimental data. Consequently, only a few donor–acceptor pairs proved suitable for a straightforward mix-and-match approach.⁹ With the use of rational design principles, donor–acceptor pairs have been covalently or topologically tethered together and thus aforementioned complications were greatly reduced.^{34–37} However, arriving at such molecules is both time-consuming and suffers from synthetic challenges when the investigation of multiple donor–acceptor pair interactions is desired and therefore often limits the scope to specific example cases. Moreover, the energetic contribution of CT to the Gibbs free binding energy cannot be obtained through a tethering strategy as the donor and acceptor have been irreversibly linked to each other. Supramolecular, noncovalent host–guest chemistry can be exploited to combine the best of both strategies compared above. First, it offers experimental ease to form the CT complex through a true mix-and-match fashion with good control over the donor–acceptor geometry at low molar concentrations. Second, it allows for the experimental thermodynamic investigation of the CT complex formation.

In this respect, cucurbit[8]uril (CB[8]), a macrocyclic, synthetic host is an ideal model system (see Figure 1a for the chemical structure). CB[8] is well-known to form selectively a 1:1:1 ternary complex with an electron-deficient, dicationic acceptor molecule such as methyl viologen MV (also known as paraquat) and an electron-rich donor such as 2,6-dihydroxynaphthalene (2,6-Np) in an aqueous environment.^{38–40} The acceptor and donor moieties are commonly referred to as first

guest (G1) and second guest (G2), respectively, as a result of their stepwise binding to the host as is depicted in Figure 1b. The ability to bind two aromatic guest molecules simultaneously in a face-to-face stacking arrangement distinguishes CB[8] from its smaller homologues CB[5]–CB[7] which typically bind only one aromatic guest moiety at a time.^{41,42} The observed high-wavelength absorption (around 560 nm) of the ternary complex CB[8]·MV·2,6-Np was immediately coined a CT absorption with its discovery.³⁹ An in-depth study by Inoue et al. was carried out on the charge-transfer interactions arising from a specific foldamer, consisting of pyridinium and dihydroxynaphthalene moieties, in both the absence and presence of different supramolecular hosts such as cyclodextrins and CB[8].⁴³ However, no systematic investigation over a range of donor–acceptor pairs within CB[8] has been conducted, in order to rule out other possible explanations for the emerging UV/vis features. On the other hand, many efforts since have been directed to exploit the CB[8] ternary complex formation as a supramolecular handcuff to design molecular machines,⁴⁴ for sensing of peptides,⁴⁵ for protein–polymer conjugation,⁴⁶ to control the formation of staggered aqueous assemblies,⁴⁷ and to induce gelation,^{48,49} to name a few. While these are important examples for the use of the CB[8] ternary complexations, the phrase “CT-driven complex formation” has been put forward while no information has been offered on the actual energetic contribution of CT interactions in the binding process.^{39,44,49} However, we have recently reported that (de)solvation effects are also of crucial importance for the Gibbs free binding energy of the CB[8] ternary self-assembly process in the aqueous phase.⁴⁰ Furthermore, strong ternary complex formation has also been observed in CB[8] systems that do not show distinct CT bands in the UV/vis.^{50,51} Herein, we investigate the existence and significance of CT interactions and other binding forces for CB[8] ternary complex formation by systematic variation of the structure and electronic properties of both donor and acceptor

guest molecules. Our results reveal that the CT interaction wavelength inside the host's cavity follows a simple correlation to the HOMO and LUMO of the donor and acceptor, respectively, in excellent agreement with the Mulliken model of CT interactions. Furthermore, we would like to encourage the experimental and theoretical scientific community to utilize the CB[8]-mediated ternary donor–acceptor complexes as a reliable model system for further in-depth study of CT interactions with a wide range of donor–acceptor combinations.

RESULTS AND DISCUSSION

Variation of the Donor and Acceptor in CB[8] Ternary Complexes. The Mulliken model of charge transfer suggests a simple dependence of the CT wavelength (λ_{max}) on the electron-affinity (E_{Aff}) of the acceptor, the ionization energy (E_{Ion}) of the donor, and an electrostatic reorganization energy (J).⁸ The scenario is depicted in Figure 1c for the ternary complex of acceptor G1, donor G2, and host CB[8] where the only contribution of the host is to “tie together” the donor and acceptor in a well-defined face-to-face stacking geometry (CB[8] has low-lying occupied and high-lying virtual orbitals and is transparent in the UV/vis >200 nm). In order to test the Mulliken model, electrochemical measurements can be invoked to obtain E_{Aff} and E_{Ion} . Alternatively, the electron affinity can be approximated by the E_{LUMO} energy of the acceptor as obtained from quantum mechanical (QM) methods whereas the ionization energy of the donor can be equated to the calculated E_{HOMO} . In this approximation, a CT process inside the host CB[8] would be confirmed if eq 1 holds true.

$$\lambda^{-1} \propto E_{\text{CT}} = E_{\text{HOMO}} - E_{\text{LUMO}} + J \quad (1)$$

However, J can neither be conveniently measured nor calculated, so that this expression cannot be directly evaluated. As it can be assumed that J is relatively constant for several structurally similar donor–acceptor pairs, we have set to measure CT λ_{max} for a wide range of viologen-type acceptors and benzene/naphthalene-type donors. This approach eliminates the need to know J directly and allows for the testing of the Mulliken model when only E_{HOMO} and E_{LUMO} are known. Noncharged aromatic molecules are typically good donors in CB[8] ternary complexes;⁴⁰ thus, various commercially available, substituted phenol and naphthol species were employed, and a listing is given in the Supporting Information Table 3. The selection has been restricted to water-soluble (≈ 1 mM) compounds to allow for ITC titrations in order to obtain direct thermodynamic information of the ternary complex formation as is described in a later section. However, if only the ternary complexes and their physical properties are of interest, also highly water-insoluble species such as anthracene can be studied as their ternary complexes with CB[8] and G1 are soluble in the submillimolar range.⁴⁰ Acceptor molecules that induce CB[8] ternary complexation are typically dicationic species, but only a few suitable examples are known at this point.^{50,52,53} Therefore, aryl-viologen derivatives shown in Figure 1a that differ in the aryl-substituent in para-position to the viologen unit, ranging from electron-donating (such as amino) to electron-withdrawing (such as nitro) moieties have been synthesized in analogy to literature procedures.⁵⁴ This design ensured that the full possible conjugation effect of the substituent can be experienced by the viologen unit and that sterical changes are kept to a

minimum. As these molecules carry a +2 charge, they were expected to be suitable first guests for CB[8], and indeed ¹H NMR, ESI-MS, UV/vis, and isothermal calorimetry (ITC) showed that they are capable of forming 1:1:1 ternary complexes with CB[8] and a suitable donor, very much similar to the known MV.³⁹ Supporting Information Figure 1 illustrates the findings for the example case of CB[8]·V–CN·2,6-Np. A three-dimensional model of the ternary complex (geometry optimized at the DFT-B3LYP/6-31G* level of theory) can be found in the Supporting Information Figure 2 and visualizes the face-to-face arrangement of the donor and acceptor in the CB[8] cavity. Some of the aryl-viologens, most notably V–Me and V–Cl, also showed a weak fluorescence that increased in intensity and blue-shifted upon complexation with CB[8], whereas the parent methyl viologen is nonfluorescent.⁵⁰ Supporting Information Figure 3 shows the situation for a 1:1:1 ternary complex of CB[8], V–Me, and tryptophan at two different excitation wavelengths. The fluorescence of the donor Trp (280 nm excitation, Supporting Information Figure 3a) was completely quenched upon ternary complex formation, which is in agreement with previous reports.^{45,46,50} Energy or charge transfer of the excited donor state to the viologen acceptor in addition to a reduction in fluorescence intensity on account of competitive light absorption of V–Me and Trp at 280 nm can explain this observation. Interestingly, the fluorescence intensity (340 nm excitation, Supporting Information Figure 3b) of CB[8]·V–Me remained unchanged upon ternary complex formation, but the emission of the acceptor species maximum red-shifted. The shift in λ_{em} points toward electrostatic/orbital interactions between the first and second guest in the ternary complex.

UV/Vis Measurements of Ternary Complexes with Various Donor–Acceptor Pairs. In an effort to verify the existence of a charge-transfer-type interaction in the CB[8] ternary complexes and to test if the observed trends in CT λ_{max} follow the prediction given by eq 1, a series of UV/vis spectra were obtained. As displayed in Figure 2, a typical intermolecular

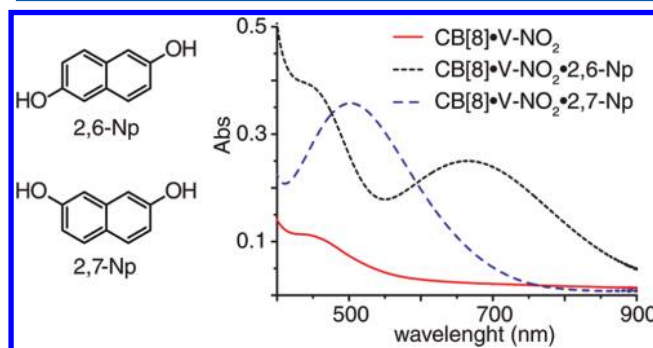


Figure 2. UV/vis spectra of CB[8]·V–NO₂, CB[8]·V–NO₂·2,6-Np, and CB[8]·V–NO₂·2,7-Np at 500 μ M conc. of each component in H₂O.

CT band centered around 665 nm can be seen for a 1:1:1 ternary complex of CB[8], V–NO₂, and 2,6-Np (see also Figure 1c). When the donor was changed to the less-conjugated 2,7-dihydroxynaphthalene (2,7-Np), a blue-shifted λ_{max} of the intermolecular CT absorption was observed. At the same time, the red-onset, which is representative of the lowest energy transition, blue-shifted as well. The UV/vis spectra of the other aryl-viologens were also recorded with 2,6-Np and with 2,7-Np as the donor molecule, consistently showing a higher CT λ_{max}

with 2,6-Np than with 2,7-Np (see Supporting Information Figures 12–19 and Supporting Information Table 3). Moreover, aryl-viologens with electron-withdrawing substituents show a more red-shifted CT λ_{max} than those with electron-donating groups, in line with the Mulliken model. There is also a very strong intramolecular CT band of the acceptor itself, here depicted for V-NH₂ as a representative example in Figure 3, that substantially red-shifts when the acceptor is

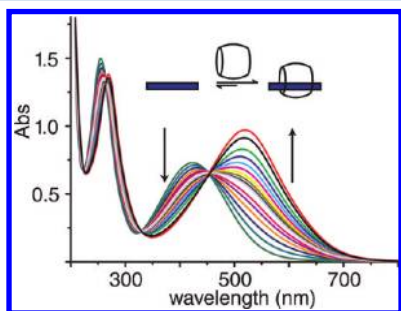


Figure 3. UV/vis titration of V-NH₂ (50 μ M) with increasing amounts of CB[8] in the direction of the arrows in H₂O.

complexed inside CB[8]. A possible explanation for the observed red-shift in the intramolecular CT band is LUMO stabilization on the viologen core upon formation of the binary CB[8]-acceptor complex. This likely occurs on account of the largely negative electrostatic potential of the CB[8] host cavity, as described in a later section, whereas the HOMOs on the aryl substituents are less influenced by the host as they sit outside the cavity. As the intramolecular CT bands begin to overlap with the intermolecular CT bands of the donor-acceptor pair with increasing electron-donating strength of the aryl-viologen substituent, we were unable to obtain the intermolecular CT λ_{max} in all cases. Thus, MV was used as an acceptor for the systematic study of the CT λ_{max} with various different donors as MV does not absorb in the visible region. As illustrated in Figure 4 for a series of para-substituted phenols, the color of



Figure 4. Ternary complexes of CB[8]·MV with para-substituted phenols (1 mM in each component, H₂O).

their ternary complexes with CB[8]·MV red-shifts with an increase in the “electron-richness” of the phenol species, again in agreement with the Mulliken model. The other donors employed and the measured CT λ_{max} for their CB[8]·MV ternary complexes are reported in Supporting Information Table 4. Supporting Information Figures 9–11 show representative UV/vis spectra.

Correlation of the Trends in CT λ_{max} with the Mulliken Model. QM calculations (DFT/B3LYP with the 6-311G* basis set for the acceptor and the 6-311+G** basis set for the donor) were carried out to obtain estimates for the acceptor LUMO and donor HOMO energies in order to test eq 1 against the experimentally obtained CT λ_{max} values. On account of computational costs, the calculations were restricted to the individual molecules (i.e., donor or acceptor) in a “vacuum” and, as such, changes in the energy levels due to polarization through the host CB[8] and due to donor-acceptor interactions were not included in this model. While the large red-shifting (98 nm) of the UV/vis intramolecular CT band in V-NH₂ upon encapsulation inside the host cavity as shown in Figure 3 indicated that CB[8] had a substantial effect on the energy level spacings of the acceptor, in a first approximation these effects should be similar for each aryl-viologen acceptor. The same reasoning applies for the donor HOMO energy levels. Despite these simplifications, a good correlation of the calculated HOMO energies to the experimentally determined λ_{max} of the intermolecular CT absorption bands for various CB[8]·MV·G2 complexes can be seen in Figure 5a, indicating

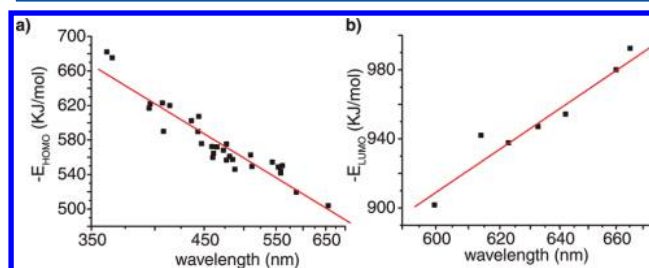


Figure 5. (a) Plot of calculated E_{HOMO} (at B3LYP/6-311G+** level of theory for vacuum geometry-optimized structures) of different second guests G2 (see Supporting Information Table 3 for details) versus measured reciprocal CT λ_{max} of CB[8]·MV·G2 in water. (b) Plot of calculated E_{LUMO} (at B3LYP/6-311G* level of theory for vacuum geometry-optimized structures) of different first guests G1 versus measured reciprocal CT λ_{max} of CB[8]·G1·2,6-Np in water. Linear fits serve to guide the eye.

that the Mulliken CT model used is applicable to this system. Moreover, there is also a good correlation of aryl-viologen acceptor E_{LUMO} to the λ_{max} shown in Figure 5b, as is predicted by eq 1.

Polarity of the CB[8] Cavity. To compare the influence of the host's cavity polarity on the CT interactions to the behavior in bulk solvents, the CT λ_{max} for the MV·2,6-Np acceptor-donor pair was measured in different polar organic solvents in the absence of CB[8]. In these cases, MV was used in combination with hexafluorophosphate counterions to ensure sufficient solubility in the organic solvents. As a ramification of the low donor-acceptor binding strength in the absence of the CB[8] host, much higher molar concentrations (~ 10 mM) of each the donor and acceptor was needed to give a CT absorbance that is comparable to that in the presence of the host. Correlation of the measured CT λ_{max} against reported Taft π^* parameters^{55,56} revealed that the CT absorption red-shifts with increasing polarity of the solvent (see Figure 6). Water does not seem to follow this correlation very well which may indicate geometry differences of the donor-acceptor complex that are induced by the different counterions (chloride vs hexafluorophosphate) or may stem from the definition of the π^* parameters. For the CT process between a noncharged

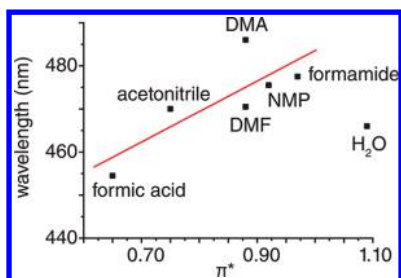


Figure 6. Correlation of measured CT wavelength for the MV·2,6-Np pair (1:1) in polar organic solvents versus their Taft π^* parameters.^{55,56} The linear fit serves to guide the eye.

aromatic donor and a dicationic viologen acceptor discussed herein, the explicitly stated charges are shown below.



Thus, the CT excited state will suffer from Coulombic repulsion which is in contrast to a conventional CT process between uncharged donors/acceptors. Polar organic solvents can serve to stabilize the CT excited state and therefore induce a red-shift in λ_{max} . Interestingly, the presence of the host CB[8] leads to an extremely red-shifted CT maximum wavelength of 560 nm for the CB[8]·MV·2,6-Np complex, i.e. a red-shift by 94 nm in comparison to water and ≥ 75 nm to the polar organic solvents employed. This is indicative of a very efficient stabilization of the CT excited state, and in this respect suggests that the CB[8] cavity is very polar. A possible explanation for this striking observation can be found in the electrostatic potential (EP) of the host. The preference of the cucurbit[n]uril ($n = 5-8, 10$) family to bind cationic species and its reluctance to complex anions had been rationalized based on the negative EP inside the cavity.⁴² The greatly uniform, negative EP within the CB[8] cavity and portal area (see Figure 7d), raises the E_{HOMO} of the electron-rich donor, relatively independently of the geometrical orientation of the donor–acceptor complex. Additionally, upon CT excitation, both donor* and acceptor* become positively charged and therefore energetically stabilized by the host's cavity. As a consequence of both effects, the CT excitation band gap will be decreased inside the host's cavity compared to the situation in solution; i.e., λ_{max} is red-shifted.

The findings described above are at first glance in contrast to polarity estimations of cucurbit[7]uril (CB[7]) by other spectroscopic techniques such as solvatochromic shifts of reporter dyes and by changes in the fluorescence intensities of molecular probes.^{57–59} These studies found that the interior of CB[7] is less polar than water but of similar or slightly higher polarity than alcohols. We believe however, that a constant, largely negative electrostatic potential represents a very unique situation, and the “large polarity” in terms of CT excited state stabilization of a $\cdot\text{G1}^{2+} \cdot \text{G2}$ acceptor–donor pair cannot be directly compared to other polarity scales. Furthermore, it has to be noted that the smaller homologues CB[5]–CB[7] show a less uniform electrostatic potential than CB[8] and have a substantially less negatively charged inner cavity than CB[8] as obtained by QM calculations (see Figure 7a–c). Unfortunately, CB[5]–CB[7] cannot accommodate two aromatic guests at a time on account of their smaller diameter, and therefore, we are unable to experimentally verify the lower “CT polarity” inside CB[5]–CB[7].

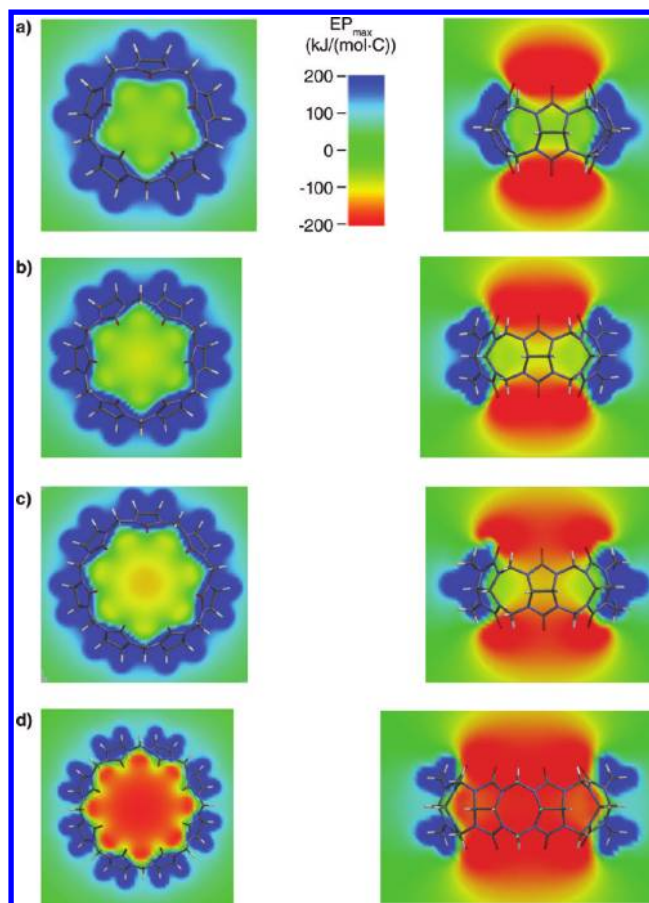


Figure 7. Calculated electrostatic potential (EP) at the B3LYP/6-31G* level of theory for (a) CB[5], (b) CB[6], (c) CB[7], and (d) CB[8] in the σ_h plane and (left) in the σ_v plane (right).

Driving Forces for CB[8] Ternary Complex Formation.

Having established that CT interactions are indeed present in ternary complexes, an estimation of the energetic importance of CT interactions for the ternary binding event was attempted. $K_{\text{aq}}(2)$, see Figure 1b for its definition, strongly depends on the desolvation penalty that G2 has to pay prior to encapsulation inside the host's cavity.⁴⁰ Specifically, less polar donor molecules were found to show much higher $K_{\text{aq}}(2)$ in aqueous solution than would be expected if CT was the most important driving force. Thus, analyzing the effect of varying the electronic properties of the acceptor (keeping G2 fixed) on the inherent driving force in $K_{\text{aq}}(2)$ for the ternary complex formation provides a better starting point to scrutinize the energetic importance of CT effects as the desolvation penalty for G1 has already been accounted for in $K_{\text{aq}}(1)$. Table 1 depicts the Gibbs free energies ($\Delta G_{\text{aq}}(2)$), enthalpies, and entropies for the ternary complex formation of CB[8]·1–CB[8]·13 with 2,6-Np as titrant as obtained by ITC measurements in aqueous solutions.

Examining the data in column 1, a clear trend is seen: The more electron-withdrawing the substituent on the aryl-viologen, the higher the association strength ($K_{\text{aq}}(2)$) of its ternary complex formation with 2,6-Np. It is worth noting that this is primarily an enthalpic effect, which could point either to a CT driving force of binding or toward electrostatic/ π – π -stacking effects. Similar thermodynamic observations were made for the structurally and sterically very different second guest

Table 1. Thermodynamic Data for the Association of the Second Guest 2,6-Np with CB[8]·G1 in H₂O at 298 K As Determined by ITC

G1	$K_{aq}(2)$ (M ⁻¹)	$\Delta G_{aq}(2)$ (kJ mol ⁻¹)	$\Delta H_{aq}(2)$ (kJ mol ⁻¹)	$-T\Delta S_{aq}(2)$ (kJ mol ⁻¹)
V-NO ₂	$(3.0 \pm 0.3) \times 10^5$	-31.3 ± 0.4	-38.9 ± 0.4	7.6 ± 0.8
V-CN	$(6.8 \pm 0.3) \times 10^5$	-33.3 ± 0.4	-50.4 ± 0.4	17.1 ± 0.8
V-F	$(2.9 \pm 0.3) \times 10^5$	-31.2 ± 0.4	-42.1 ± 0.4	10.9 ± 0.8
V-CO ₂ Et	$(9.4 \pm 0.3) \times 10^5$	-34.1 ± 0.4	-44.6 ± 0.4	10.5 ± 0.8
V-Cl	$(9.3 \pm 0.2) \times 10^4$	-28.4 ± 0.3	-27.6 ± 0.4	-0.8 ± 0.7
V-Br	$(1.8 \pm 0.3) \times 10^5$	-30.0 ± 0.4	-27.5 ± 0.4	-2.5 ± 0.8
V-H	$(2.3 \pm 0.2) \times 10^4$	-24.9 ± 0.3	-12.9 ± 0.4	-11.9 ± 0.8
V-I	$(2.1 \pm 0.3) \times 10^5$	-30.3 ± 0.4	-24.3 ± 0.4	-6.0 ± 0.8
V-Me	$\leq 1.0 \times 10^3$	≥ -17	— ^a	— ^a
V-OMe	$(1.3 \pm 0.3) \times 10^3$	-17.8 ± 0.4	— ^a	— ^a
V-NH ₂	$(2.9 \pm 0.4) \times 10^3$	-19.7 ± 0.4	— ^a	— ^a

^aIsotherm is not suitable for fitting of accurate $\Delta H_{aq}(2)$ and $\Delta S_{aq}(2)$.

2-methoxydibenzofuran (DBF) that has been covalently linked to a poly(ethylene glycol) polymer (PEG) (see Supporting Information Table 2 and Figure 4). In contrast to these findings, no clear trends in $K_{aq}(1)$ can be observed for the first binding equilibria of CB[8] with the aryl-viologens, likely on account of overlaying desolvation effects (see Supporting Information Table 1). Furthermore, ESI-MS experiments on 1:1:1 aqueous solutions of CB[8], G1, and 2,6-Np have been employed to get an understanding of the *inherent* ternary complex stabilities, i.e., in the absence of solvation effects. Since eq 3 would hold true if a gas-phase equilibrium were established under ESI-MS conditions, the logarithmic ratio of the ESI-MS peak intensities of the ternary to the binary complex ($\ln([CB[8] \cdot G1 \cdot 2,6-Np] \times [CB[8] \cdot G1]^{-1})$) was used as a measure for the gas-phase stability of the ternary complexes.

$$\begin{aligned} \Delta G_{vac} &\propto \ln(K_{vac}) \\ &\propto \ln([CB[8] \cdot G1 \cdot 2,6-Np] \times [CB[8] \cdot G1]^{-1} \\ &\quad \times [2,6-Np]^{-1}) \end{aligned} \quad (3)$$

There is a good correlation of the $\Delta G_{aq}(2)$ from aqueous solutions to the above-defined logarithmic ratio of the ESI-MS intensities when the acceptor is varied as is shown in Supporting Information Figure 5. In contrast to this finding, aqueous and gas-phase ternary binding strength do not correlate at all when the donor is changed.⁴⁰ The latter can be rationalized by the significant energetic effect of the donor desolvation on $\Delta G_{aq}(2)$. We had reported that the ESI-MS stabilities rank with a quantity $\Delta G_{vac}(2)$ that was defined as $\Delta G_{vac}(2) = \Delta G_{aq}(2) + \Delta G_{solv}(G2)$, where $\Delta G_{solv}(G2)$ is the solvation free energy of the donor.⁴⁰ In other words, comparing $\Delta G_{vac}(2)$ for different donors gives an estimate of their relative binding affinity for CB[8]·G1 where the desolvation penalty of the second guest has been accounted for.

These obtained gas-phase stabilities for the variation of the donor and of the acceptor were then tested against two possible hypotheses: (1) the ternary complex is CT-driven, or (2) it is governed by electrostatic/ π - π -stacking effects. If the ternary complexation is CT-driven, a correlation of the binding affinities with the E_{HOMO}/E_{LUMO} was expected, whereas electrostatic effects should lead to correlation with the electrostatic potential (EP). EP maps were employed to visualize and quantify the electrostatic charge distribution of the acceptor and donor. In Figure 8b, three representative EP maps for the aryl-viologens V-Me, V-NH₂, and V-NO₂ are

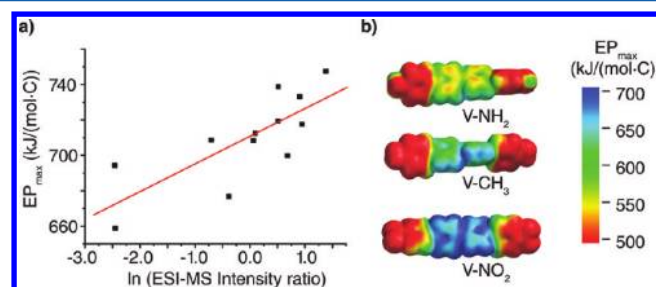


Figure 8. (a) Correlation of the calculated (B3LYP/6-311G*) maximum electrostatic potential EP_{max} on the viologen versus logarithmic ratio of ESI-MS intensities $\ln([CB[8] \cdot G1 \cdot 2,6-Np] \times [CB[8] \cdot G1]^{-1})$ for the series of viologen derivatives. The linear fit serves to guide the eye. (b) Electrostatic potential maps of V-NH₂, V-CH₃, and V-NO₂ at B3LYP/6-311G* level of theory. The same color scale was used for each electrostatic property map on an isodensity surface.

shown. It is evident that the doubly cationic charge is localized on the bipyridinium core when electron-withdrawing substituents (such as nitro) are present, whereas the EP is substantially reduced on the core when electron-donating substituents (such as amino) are attached to the aryl-moieties. The maximum electrostatic potential value (EP_{max}) on the bipyridinium isodensity surface was taken as a measure for the electrostatic properties of the whole molecule. We further confirmed that this is a suitable procedure as an average EP taken from many points on the viologen core shows an excellent correspondence with the EP_{max} . These calculated values were then compared to the experimentally determined binding affinities. For the variation of the acceptor, there is a good correlation between EP_{max} values of the aryl-viologen with the gas-phase stability of the ternary complex, as shown in Figure 8a. A higher EP of the aryl-viologen should lead to stronger electrostatic interaction with the electron-rich donor as well as with the negatively charged host cavity, in line with the experimental findings. A slightly worse correlation exists between EP_{max} and the Gibbs free energy $\Delta G_{aq}(2)$ in aqueous solution (see Supporting Information Figure 6), again pointing toward the complicating effects caused by (de)solvation. Unfortunately, the energetic importance of CT effects and electrostatic interactions cannot be distinguished when varying the structure of the acceptor, because the aryl-viologen derivatives also display an excellent direct proportionality between the calculated EP_{max} and the calculated E_{LUMO} , as is depicted in Supporting Information Figure 7.

When varying the donor structure, there is no correlation of $\Delta G_{\text{vac}}(2)$ with either the average EP of the donor or with its E_{HOMO} (see Supporting Information Figure 8). As expected, also $\Delta G_{\text{aq}}(2)$ shows no trends with the EP and E_{HOMO} energy as solvation effects serve to further complicate the picture. Moreover, no correlation of $\Delta G_{\text{vac}}(2)$ with the EP or E_{HOMO} can be observed even if only a subset of donors such as para-substituted phenols or isomeric dihydroxynaphthalenes were compared to keep the steric effects similar within the donor series. The lack of correlation of the aqueous and gas-phase binding free energies with the E_{HOMO} clearly points to the fact that neither in aqueous solution nor when solvation effects are accounted for is there any evidence for a “CT-driven ternary complex formation”, in contrast to the claims present in the CB[8] literature.^{39,44,49} However, the absence of a simple correlation of $\Delta G_{\text{vac}}(2)$ with the EP of the donor had to be expected and is not in conflict with the electrostatic/ π – π -stacking model. One must remember that the cavity of the host has a largely negative EP whereas the acceptor possesses a largely positive EP. Consequently, the second guest must balance the electrostatic repulsion/attraction to both the host and G1, which leads to the complicated overall behavior seen.

CONCLUSIONS

In conclusion, the spectroscopic features of cucurbit[8]uril-mediated ternary complexes have been investigated by variation of both the acceptor and donor properties of the first and second guests, respectively. A good proportionality between the reciprocal CT maximum wavelength and the E_{LUMO} of the acceptor as well as the E_{HOMO} of the donor was found and provides compelling evidence for the existence of charge-transfer interactions in CB[8]-ternary complexes, in good agreement with the classical CT model by Mulliken. It has also been shown that the CT excited state is likely much more stabilized inside the CB[8] cavity than in a solution environment. This surprising finding can be rationalized by the largely negative but rather uniform electrostatic potential inside the host cavity. On the other hand, no evidence in both aqueous medium and “gas-phase” could be found for CT interactions being of significant importance to the Gibbs binding free energies of the ternary complexes. Therefore, the concept of a “CT-driven ternary complexation” should be revisited. The well-defined face-to-face stacking geometry of the donor–acceptor pair as well as their high binding affinity to each other in the presence of the host makes CB[8] ternary complexes an ideal model system for further studies of CT interactions and should be of interest for the physicochemical and theoretical communities.

EXPERIMENTAL SECTION

Materials. See Supporting Information for detailed experimental procedures, ITC, and ESI-MS measurements.

ASSOCIATED CONTENT

Supporting Information

Detailed synthetic procedures, UV/vis, NMR, and ESI-MS spectra, and ITC plots. This material is available free of charge via the Internet at <http://pubs.acs.org>.

AUTHOR INFORMATION

Corresponding Author

*E-mail: oas23@cam.ac.uk.

Notes

The authors declare no competing financial interest.

ACKNOWLEDGMENTS

F.B. thanks the German Academic Exchange Service (DAAD) for financial support.

REFERENCES

- (1) Sheps, L.; Miller, E. M.; Horvath, S.; Thompson, M. A.; Parson, R.; McCoy, A. B.; Lineberger, W. C. *Science* **2010**, 328, 220–224.
- (2) D'Alessandro, D. M.; Keene, F. R. *Chem. Soc. Rev.* **2006**, 35, 424–440.
- (3) Li, R.; Zheng, J.; Truhlar, D. G. *Phys. Chem. Chem. Phys.* **2010**, 12, 12697–12701.
- (4) Vogler, A.; Kunkely, H. *Coord. Chem. Rev.* **2004**, 248, 273–278.
- (5) Kysel, O.; Budzak, S.; Mach, P.; Medved, M. *Int. J. Quantum Chem.* **2010**, 110, 1712–1728.
- (6) Solis, C.; Grosso, V.; Faggioli, N.; Cosa, G.; Romero, M.; Previtali, C.; Montejano, H.; Chesta, C. *Photochem. Photobiol. Sci.* **2010**, 9, 675–686.
- (7) Hu, N.; Tu, Y.-P.; Jiang, K.; Pan, Y. *J. Org. Chem.* **2010**, 75, 4244–4250.
- (8) Mulliken, R. S. *J. Am. Chem. Soc.* **1950**, 72, 600–608.
- (9) Levy, D.; Arnold, B. R. *J. Am. Chem. Soc.* **2004**, 126, 10727–10731.
- (10) Ahn, T. K.; Avenson, T. J.; Ballottari, M.; Cheng, Y.-C.; Niyogi, K. K.; Bassi, R.; Fleming, G. R. *Science* **2008**, 320, 794–797.
- (11) Bombarda, E.; Ullmann, G. M. *Faraday Discuss.* **2011**, 148, 173–193.
- (12) Driscoll, K.; Fang, J.; Humphry-Baker, N.; Torres, T.; Huck, W. T. S.; Snaith, H. J.; Friend, R. H. *Nano Lett.* **2010**, 10, 4981–4988.
- (13) Aziz, E.; Vollmer, A.; Eisebitt, S.; Eberhardt, W.; Pingel, P.; Neher, D.; Koch, N. *Adv. Mater.* **2007**, 19, 3257–3260.
- (14) Peng, H.; Ran, C.; Yu, X.; Zhang, R.; Liu, Z. *Adv. Mater.* **2005**, 17, 459–464.
- (15) Bredas, J.-L.; Beljonne, D.; Coropceanu, V.; Cornil, J. *Chem. Rev.* **2004**, 104, 4971–5004.
- (16) Ren, L.; Xian, X.; Yan, K.; Fu, L.; Liu, Y.; Chen, S.; Liu, Z. *Adv. Funct. Mater.* **2010**, 20, 1209–1223.
- (17) Wang, W.; Yan, D.; Bratton, D.; Howdle, S. M.; Wang, Q.; Lecomte, P. *Adv. Mater.* **2003**, 15, 1348–1352.
- (18) Tahara, K.; Fujita, T.; Sonoda, M.; Shiro, M.; Tobe, Y. *J. Am. Chem. Soc.* **2008**, 130, 14339–14345.
- (19) Wang, C.; Guo, Y.; Wang, Y.; Xu, H.; Wang, R.; Zhang, X. *Angew. Chem., Int. Ed.* **2009**, 48, 8962–8965.
- (20) Murata, T.; Morita, Y.; Fukui, K.; Sato, K.; Shiomi, D.; Takui, T.; Maesato, M.; Yamochi, H.; Saito, G.; Nakasuji, K. *Angew. Chem., Int. Ed.* **2004**, 43, 6343–6346.
- (21) Schneider, H.-J.; Yatsimirsky, A. K. *Chem. Soc. Rev.* **2008**, 37, 263–277.
- (22) Meyer, E. A.; Castellano, R. K.; Diederich, F. *Angew. Chem., Int. Ed.* **2003**, 42, 1210–1250.
- (23) Hunter, C. A.; Sanders, J. K. M. *J. Am. Chem. Soc.* **1990**, 112, 5525–5534.
- (24) Jones, J. T. A.; Hasell, T.; Wu, X.; Bacsá, J.; Jelfs, K. E.; Schmidtman, M.; Chong, D. J.; Adams, S. Y.; Trewin, A.; Schiffman, F.; Cora, F.; Slater, B.; Steiner, A.; Day, G. M.; Cooper, A. I. *Nature* **2011**, 474, 367–371.
- (25) Reczek, J. J.; Iverson, B. L. *Macromolecules* **2006**, 39, 5601–5603.
- (26) McKinlay, R.; Atwood, J. *Angew. Chem., Int. Ed.* **2007**, 46, 2394–2397.
- (27) Bruckner, R. C.; Zhao, G.; Ferreira, P.; Jorns, M. S. *Biochemistry* **2006**, 46, 819–827.
- (28) Efimov, I.; McIntire, W. S. *J. Am. Chem. Soc.* **2004**, 127, 732–741.

- (29) Regeimbal, J.; Gleiter, S.; Trumpower, B. L.; Yu, C.-A.; Diwakar, M.; Ballou, D. P.; Bardwell, J. C. A. *Proc. Natl. Acad. Sci. U.S.A.* **2003**, *100*, 13779–13784.
- (30) Gonzalez-Bejar, M.; Stiriba, S.-E.; Miranda, M. A.; Perez-Prieto, J. *Org. Lett.* **2007**, *9*, 453–456.
- (31) Saito, H.; Mori, T.; Wada, T.; Inoue, Y. *J. Am. Chem. Soc.* **2004**, *126*, 1900–1906.
- (32) Asaoka, S.; Wada, T.; Inoue, Y. *J. Am. Chem. Soc.* **2003**, *125*, 3008–3027.
- (33) Imai, Y.; Kido, S.; Kamon, K.; Kinuta, T.; Sato, T.; Tajima, N.; Kuroda, R.; Matsubara, Y. *Org. Lett.* **2007**, *9*, 5047–5050.
- (34) Stephenson, R. M.; Wang, X.; Coskun, A.; Stoddart, J. F.; Zink, J. I. *Phys. Chem. Chem. Phys.* **2010**, *12*, 14135–14143.
- (35) Kwan, P. H.; Swager, T. M. *J. Am. Chem. Soc.* **2005**, *127*, 5902–5909.
- (36) Nygaard, S.; Hansen, S. W.; Huffman, J. C.; Jensen, F.; Flood, A. H.; Jeppesen, J. O. *J. Am. Chem. Soc.* **2007**, *129*, 7354–7363.
- (37) Hariharan, M.; Karunakaran, S. C.; Ramaiah, D. *Org. Lett.* **2007**, *9*, 417–420.
- (38) Kim, J.; Jung, I. S.; Kim, S. Y.; Lee, E.; Kang, J. K.; Sakamoto, S.; Yamaguchi, K.; Kim, K. *J. Am. Chem. Soc.* **2000**, *122*, 540–541.
- (39) Kim, H.-J.; Heo, J.; Jeon, W. S.; Lee, E.; Kim, J.; Sakamoto, S.; Yamaguchi, K.; Kim, K. *Angew. Chem., Int. Ed.* **2001**, *40*, 1526–1529.
- (40) Rauwald, U.; Biedermann, F.; Deroo, S.; Robinson, C. V.; Scherman, O. A. *J. Phys. Chem. B* **2010**, *114*, 8606–8615.
- (41) Lee, J. W.; Samal, S.; Selvapalam, N.; Kim, H. J.; Kim, K. *Acc. Chem. Res.* **2003**, *36*, 621–630.
- (42) Lagona, J.; Mukhopadhyay, P.; Chakrabarti, S.; Isaacs, L. *Angew. Chem., Int. Ed.* **2005**, *44*, 4844–4870.
- (43) Mori, T.; Ko, Y. H.; Kim, K.; Inoue, Y. *J. Org. Chem.* **2006**, *71*, 3232–3247.
- (44) Ko, Y. H.; Kim, E.; Hwang, I.; Kim, K. *Chem. Commun.* **2007**, 1305–1315.
- (45) Bush, M. E.; Bouley, N. D.; Urbach, A. R. *J. Am. Chem. Soc.* **2005**, *127*, 14511–14517.
- (46) Biedermann, F.; Rauwald, U.; Zayed, J. M.; Scherman, O. A. *Chem. Sci.* **2011**, *2*, 279–286.
- (47) Jiao, D.; Biedermann, F.; Tian, F.; Scherman, O. A. *J. Am. Chem. Soc.* **2010**, *132*, 15734–15743.
- (48) Appel, E. A.; Biedermann, F.; Rauwald, U.; Jones, S. T.; Zayed, J. M.; Scherman, O. A. *J. Am. Chem. Soc.* **2010**, *132*, 14251–14260.
- (49) Liu, Y.; Yu, Y.; Gao, J.; Wang, Z.; Zhang, X. *Angew. Chem., Int. Ed.* **2010**, *49*, 6576–6579.
- (50) Biedermann, F.; Rauwald, U.; Cziferszky, M.; Williams, K. A.; Gann, L. D.; Guo, B. Y.; Urbach, A. R.; Bielawski, C. W.; Scherman, O. A. *Chem.—Eur. J.* **2010**, *16*, 13716–13722.
- (51) Jiao, D.; Biedermann, F.; Scherman, O. A. *Org. Lett.* **2011**, *13*, 3044–3047.
- (52) Sindelar, V.; Cejas, M. A.; Raymo, F. M.; Chen, W.; Parker, S. E.; Kaifer, A. E. *Chem.—Eur. J.* **2005**, *11*, 7054–7059.
- (53) Ling, Y.; Wang, W.; Kaifer, A. E. *Chem. Commun.* **2007**, *6*, 610–612.
- (54) Bongard, D.; Möller, M.; Rao, S. N.; Corr, D.; Walder, L. *Helv. Chim. Acta* **2005**, *88*, 3200–3209.
- (55) Marcus, Y. *Chem. Soc. Rev.* **1993**, *22*, 409–416.
- (56) Kamlet, M. J.; Abboud, J. L. M.; Abraham, M. H.; Taft, R. W. *J. Org. Chem.* **1983**, *48*, 2877–2887.
- (57) Nau, W. M.; Florea, M.; Assaf, K. I. *Isr. J. Chem.* **2011**, *51*, 559–577.
- (58) Mohanty, J.; Nau, W. M. *Angew. Chem., Int. Ed.* **2005**, *44*, 3750–3754.
- (59) Rankin, M. A.; Wagner, B. D. *Supramol. Chem.* **2004**, *16*, 513–519.